Supporting Information

Preparation of Antibacterial Polypeptides with Different Topologies and Their Antibacterial Properties

Xiaodan Wang,[a, b] Fangping Yang,[c] Huawei Yang,[*a, b] Xu Zhang,[a] Haoyu Tang[*c] and Shifang Luan [a, b]

[a] State Key Laboratory of Polymer Physics and Chemistry, Changchun Institute of Applied Chemistry, Chinese Academy of Sciences, Changchun 130022, P.R. China

[b] University of Science and Technology of China, Hefei 230026, P. R. China

[c] Institute of Functional Nano & Soft Materials (FUNSOM), Collaborative Innovation Center of Suzhou Nano Science & Technology, Soochow University, 199 Ren'ai Road, Suzhou, 215123, Jiangsu, PR China

* Corresponding author

Huawei Yang (E-mail: yanghw@ciac.ac.cn) or Haoyu Tang (E-mail: hytang@suda.edu.cn).

Instrumentation

^{1}H nuclear magnetic resonance spectroscopy (^{1}H-NMR)：^{1}H-NMR was performed on a Bruker AV 400 MHz spectrometer. Chemical shifts (δ) were reported in the units of ppm and referenced to the TMS.

Fourier transform-infrared spectroscopy (FTIR): FTIR was recorded on a BRUKER Vertex 70 in the range of 400–4000 cm^{-1}. Total of 32 scans were accumulated with a resolution of 4 cm^{-1} for each spectrum.

Gel permeation chromatography (GPC): GPC was performed on a system equipped with an isocratic pump (Model 1100, Agilent Technology, Santa Clara, CA, USA), a DAWN HELEOS multi-angle laser light scattering detector (MALLS) detector (Wyatt Technology, Santa Barbara, CA, USA), and an Optilab rEX refractive index detector (Wyatt Technology, Santa Barbara, CA, USA). The detection wavelength of HELEOS was set at 658 nm. Separations were performed using serially connected size exclusion columns (100 Å, 500 Å, 10^3 Å and 10^4 Å Phenogel columns, 5 μm, 300 × 7.8 mm, Phenomenex, Torrance, CA, USA) at 60 °C using DMF containing 0.05 M LiBr as the eluent phase at a flow rate of 1.0 mL min^{-1}.

Mass spectrometry (MS): The purity of Gx-PAMAM were confirmed by MS (Bruker Daltonics flexAnalysis). The samples were dissolved in DMF to obtain a solution with a concentration of 1 mg mL^{-1} for testing.

Circular dichroism (CD)：CD measurements were carried out on a JASCO J-700 CD spectrometer. The AMPs solution with a concentration of 0.2 mg mL^{-1} in 10 mM PBS buffer was filled in a quartz cell with a path length of 0.1 cm. Three scans were performed and averaged between 190-250 nm by subtracting the solvent background. The CD spectra were expressed in mean residue ellipticity (MRE, $[\theta]_\lambda$ in deg cm^2 dmol^{-1}) which was calculated by the following equation:

$$[\theta]_\lambda = \text{MRW} \times \theta_\lambda / 10 \times d \times c,$$

where MRW is the mean residue weight (here refers to the molecular weight of polypeptide repeating unit), θ_λ is the observed ellipticity (mdeg) at the wavelength λ, d is the path length (mm) and c is the concentration (mg mL^{-1}) of the AMPs.[1] The relative helical content, namely the fractional helicity (f_H) was calculated based on the mean residue ellipticity at 222 nm:

$$f_H = (-[\theta]_{222} + 3{,}000)/39{,}000.[2]$$

Dynamic light scattering (DLS)：DSL and zeta potential were measured on a Zetasizer Nano ZS90 (Malvern Instruments, Ltd., UK) with a He-Ne laser ($\lambda = 633$ nm) at a scattering angle of 90° (25 °C). Measurements were performed at concentrations of 1 mg mL^{-1} in 10 mM PBS buffer. All samples were filtered through 0.45 μm nylon filters before measurement.

Transmission electron microscope (TEM): The assembled structure of the AMPs in solution was observed by TEM (JEM-1400 Flash). The AMPs were dissolved in 10 mM PBS buffer with a concentration of 1 mg mL^{-1}, then a droplet of 5 μL of the above solution was added on the T11023 formvar carbon coated grids, followed by air drying at room temperature for observation.

X-ray photoelectron spectroscopy (XPS, VG Scientific ESCA MK II Thermo Avantage V3.20 analyzer equipped with an Al Kα anode mono-X-ray source, hv= 1486.6 eV) was adopted to study the surface composition. Data treatment was analyzed with the XPSPEAK Version 4.0 software.

Atomic force microscope (AFM): Surface morphology and roughness were characterized by AFM (SPA300HV with a SPI 3800 controller, Seiko Instruments Industry, Japan) with contact mode. The root-mean-square (RMS) roughness was evaluated directly from AFM images.

Water contact angles (WCAs) of the surfaces were measured by a sessile-drop method in air with a drop shape analysis instrument (DSA, KRÜSS GMBH, Hamburg 100) at room temperature. For each sample, a 2 μL water droplet was dropped each time and at least five places were measured for calculating the average value.

Scanning electron microscopy (SEM): The cellular morphologies of the bacteria attached on surface were acquired by SEM (XL 30 FESEM FEG, FEI Company, USA, at an accelerating voltage of 10 kV). Before imaging, the prepared samples were sputter-coated with gold palladium.

Confocal laser-scanning microscope (CLSM): The cellular activities of the bacteria on surface were measured by CLSM (LSM 700, Carl Zeiss). The samples were dyed with LIVE/DEAD Baclight Bacterial Viability Kit (L-7012) according to the manufacturer's procedure.

Preparation and Characterization of the NCAs.

Synthesis of Boc-L-Lys-NCA: H-Lys(Boc)-OH (10.0 g, 40.6 mmol) was suspended in 180 mL of THF in a round bottom flask at 50 °C, followed by addition of a solution of triphosgene (4.4 g, 14.9 mmol) in THF (20 mL). The reaction media clarified around 10 min after the complete addition of triphosgene. Then the reaction mixture was cooled to room temperature, and the solvent was removed by rotary evaporation to yield a crude product, which was recrystallized three times using ethyl acetate and hexane to yield a white powder (5.1 g, 46.1% yield). ^{1}H NMR (400 MHz, DMSO-d_6) δ (ppm): 9.06 (s, 1H-*1.00*, -CON*H*CH-), 6.77 (t, 1H-*1.00*, -CH$_2$N*H*COO-), 4.46–4.36 (m, 1H-*1.00*, -NHC*H*CH2-), 2.90 (q, 2H-*2.05*, -CHC*H$_2$*CH$_2$-), 1.81–1.58 (m, 2H-*2.05*, -C*H$_2$*NHCOO-), 1.39–1.22 (m, 13H-*13.45*, -C*H$_2$CH$_2$*CH$_2$NHCOOC*(CH$_3$)$_3$*).

Synthesis of D-Phe-NCA: A solution of triphosgene (6.60 g, 22.2 mmol) in THF (20 mL) was added into 10.0 g of D-Phe (60.5 mmol) that was pre-dispersed in THF (180 mL) in a round bottom flask at 50 °C. The mixture was stirred vigorously until the solution became clear (approximately 60 min). White powdery product (6.2 g, 53.6%

yield) was obtained after three recrystallizations from ethyl acetate/hexane. ^{1}H NMR (400 MHz, CDCl$_3$) δ (ppm): 7.43–7.03 (m, 5H-*5.47*, **Ar*H*CH2-**), 6.38 (s, 1H-*1.00*, -CON*H*CH-), 4.53 (dd, 1H-*1.10*, -NHC*H*CH2-), 3.25 (dd, 1H-*1.10*, ArC*H$_2$*CH-), 3.01 (dd, 1H-*1.10*, ArC*H$_2$*CH-).
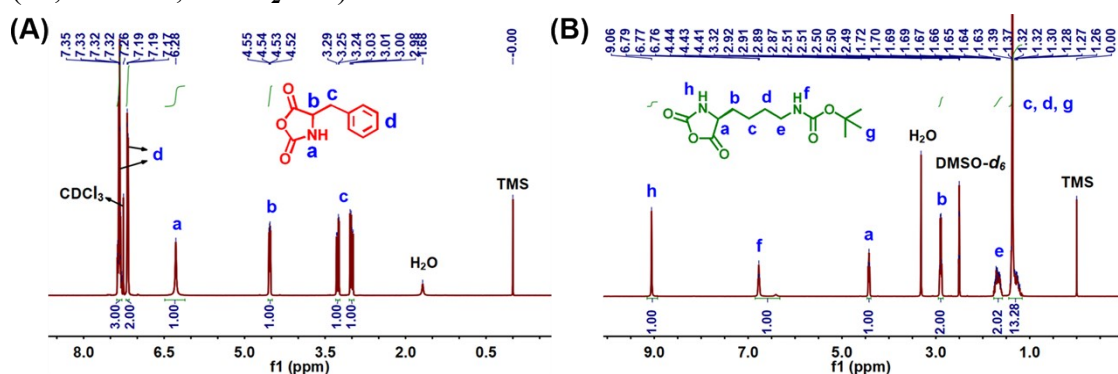

Figure S1. ^{1}H NMR spectra of (A) L-BOC-Lys-NCA and (B) D-Phe-NCA.

Table 1. The feeds of all polymers and their yields before and after deprotection.

Sample-K content (%)	L$_1$-70	L$_2$-60	L$_3$-50	G$_{1-1}$-70	G$_{1-2}$-60	G$_{1-3}$-50	G$_{2-1}$-70	G$_{2-2}$-60	G$_{2-3}$-50
Boc-L-Lys-NCA mg (mmol)	381.2 (1.4)	326.8 (1.2)	272.3 (1.2)	381.2 (1.4)	326.8 (1.2）	272.3 (1.2)	381.2 (1.4)	326.8 (1.2）	272.3 (1.2)
D-Phe-NCA mg (mmol)	114.7 (0.6)	153.0 (0.8)	191.2 (1.0)	114.7 (0.6)	153.0 (0.8)	191.2 (1.0)	114.7 (0.6)	153.0 (0.8)	191.2 (1.0)
Initiator μL(μmol)	445 (66.7)	445 (66.7)	445 (66.7)	400 (8.4)	400 (8.4)	400 (8.4)	200 (4.2)	200 (4.2)	200 (4.2)
Yield (before/after deprotection) (%)	82.0/ 84.5	85.3/ 88.4	88.4/ 92.1	89.3/ 83.8	90.9/ 83.8	93.1/ 83.8	85.6/ 83.8	87.0/ 83.8	89.3/ 83.8

Before polymerization, the purity of the Gx-PAMAM initiators were checked by MALDI-TOF MS (Figure S2&S3). Tentative experiments showed that the impurity in the Gx-PAMAM, i.e., low generation side products, could cause the multi-peak dispersity of the AMPs (Figure S8A-B). Therefore, the Gx-PAMAM initiators with high purity (according to MALDI-TOF) were used for the subsequent NCA polymerization. Previous studies[3, 4] points out that the polymerization of NCAs has a self-catalysis feature when employing solvents with low dielectric constants. With this in mind, THF (ε=7.58) instead of commonly used DMF (ε=37.6) was chosen as the solvent in this study. GPC analysis (Figure S8C-D) showed that polymerization in THF were more controllable than it in DMF, which was consistent with previous reports[5, 6] that attributed the superiority of THF to the higher stability of NCAs in this solvent than in DMF.
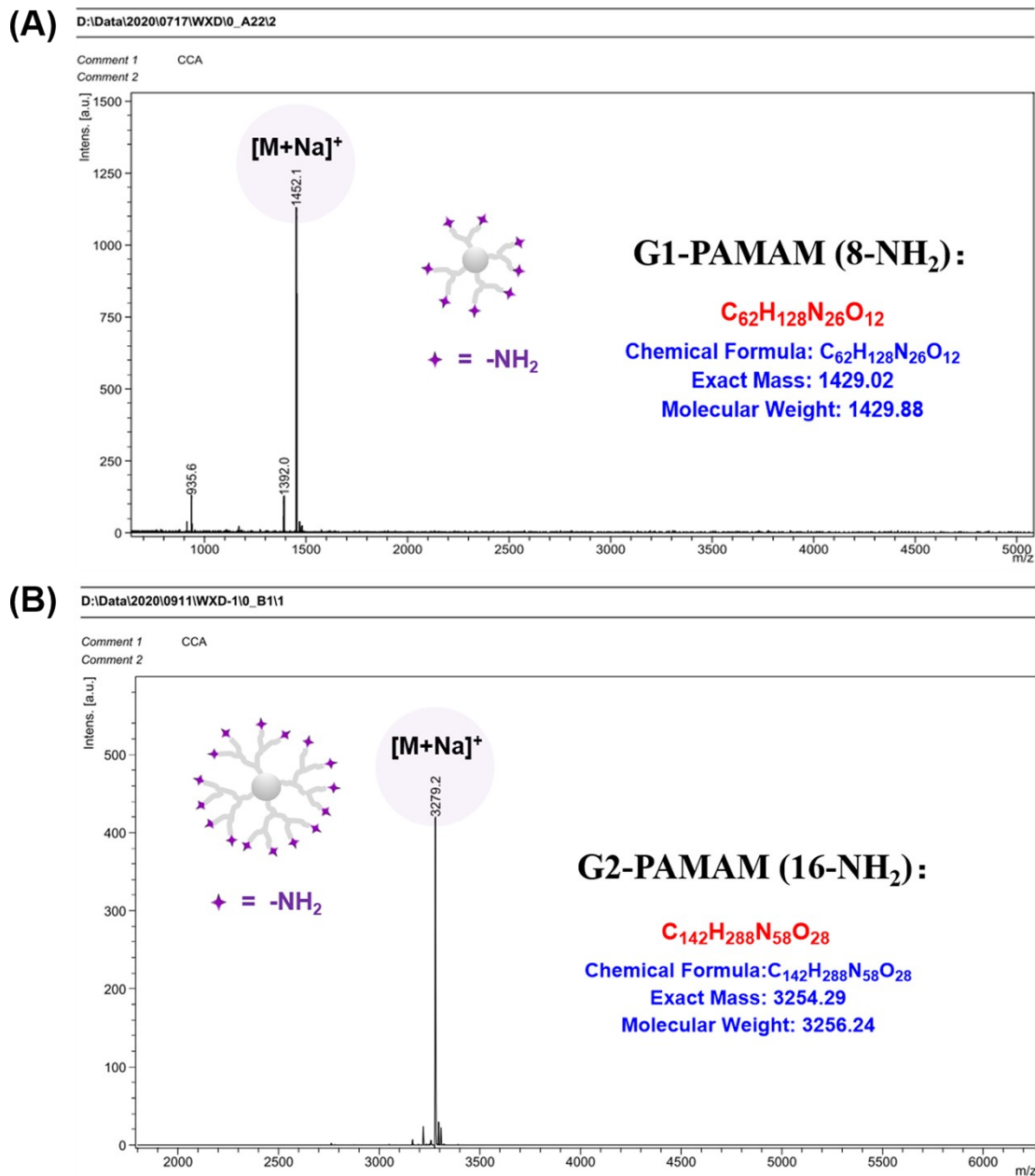
Figure S2. MALDI-TOF MS spectra of pure (A) G_1-PAMAM and (B) G_2-PAMAM for synthesis of star-shaped AMPs.
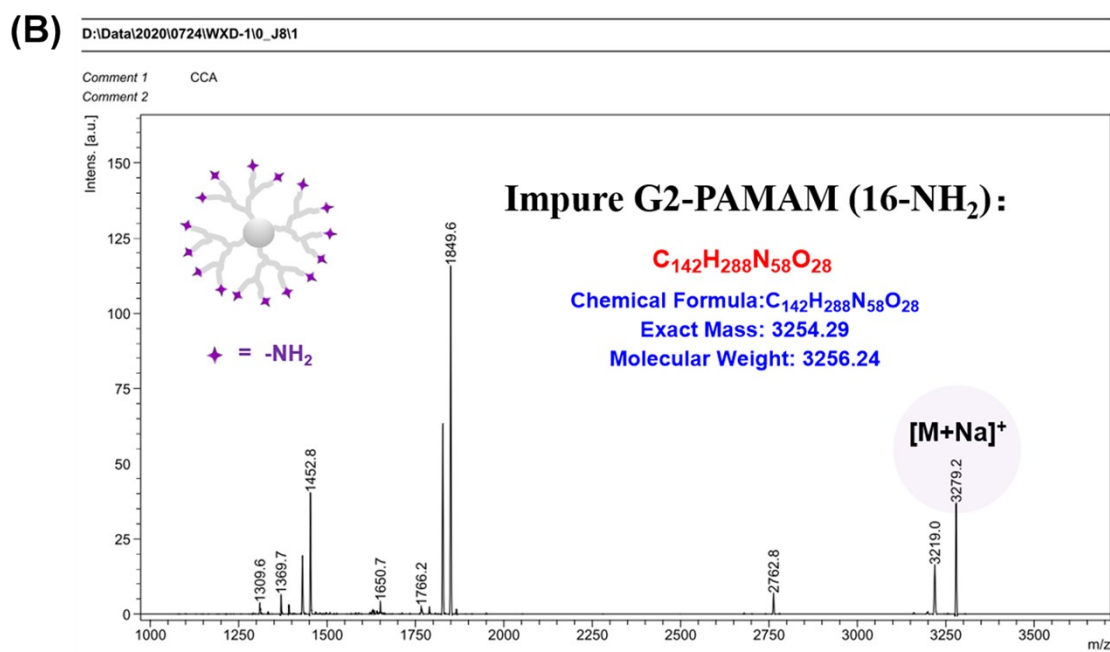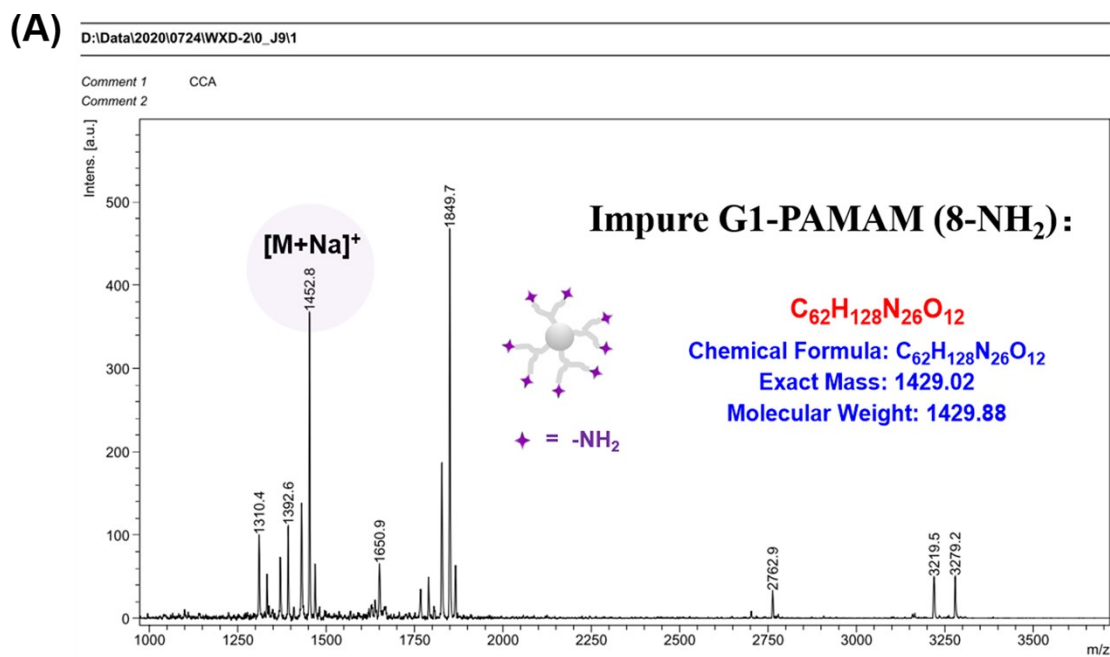
Figure S3. MALDI-TOF MS spectra of Impure (A) G_1-PAMAM and (B) G_2-PAMAM.
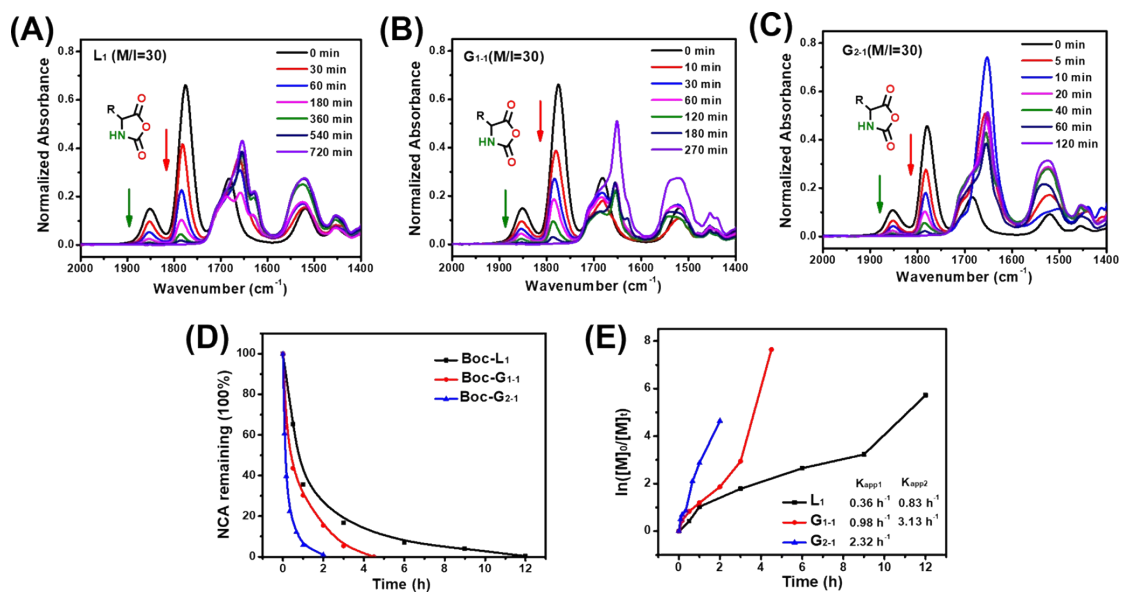
Figure S4. The conversion of monomers initiated by (A) n-hexylamine (B) G_1-PAMAM, and (C) G_2-PAMAM at different time points monitored by FTIR. (D) The NCA remaining percent calculated by the absorption at 1852 cm^{-1}. (E) Polymerization rate of the n-butylamine and Gx-PAMAM initiated ROP in THF.
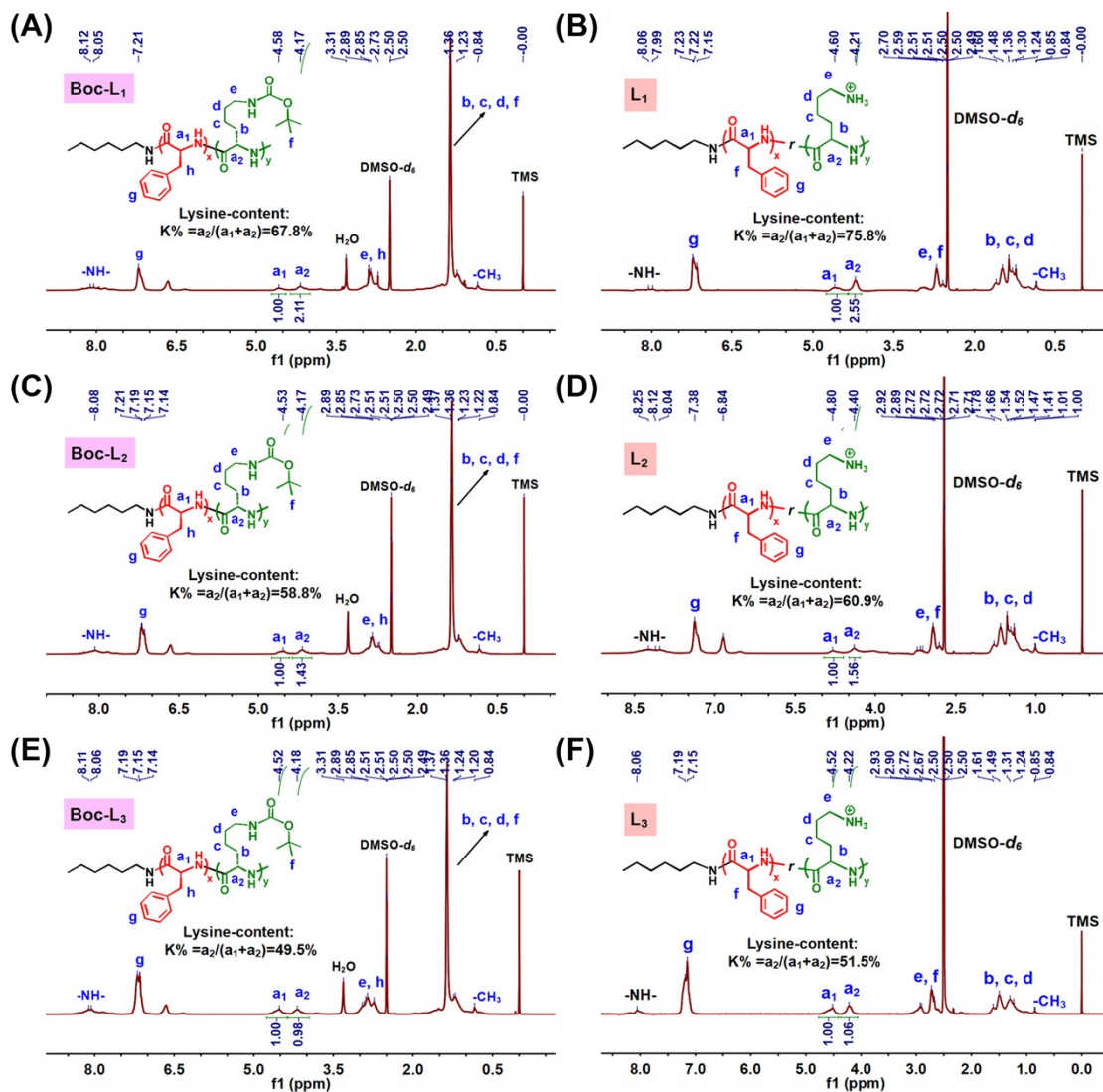
Figure S5. ^{1}H NMR spectra of linear AMPs before and after protection. (A) Boc-L_1; (B) Boc-L_2; (C) Boc-L_3; (D) L_1; (E) L_2; (F) L_3.
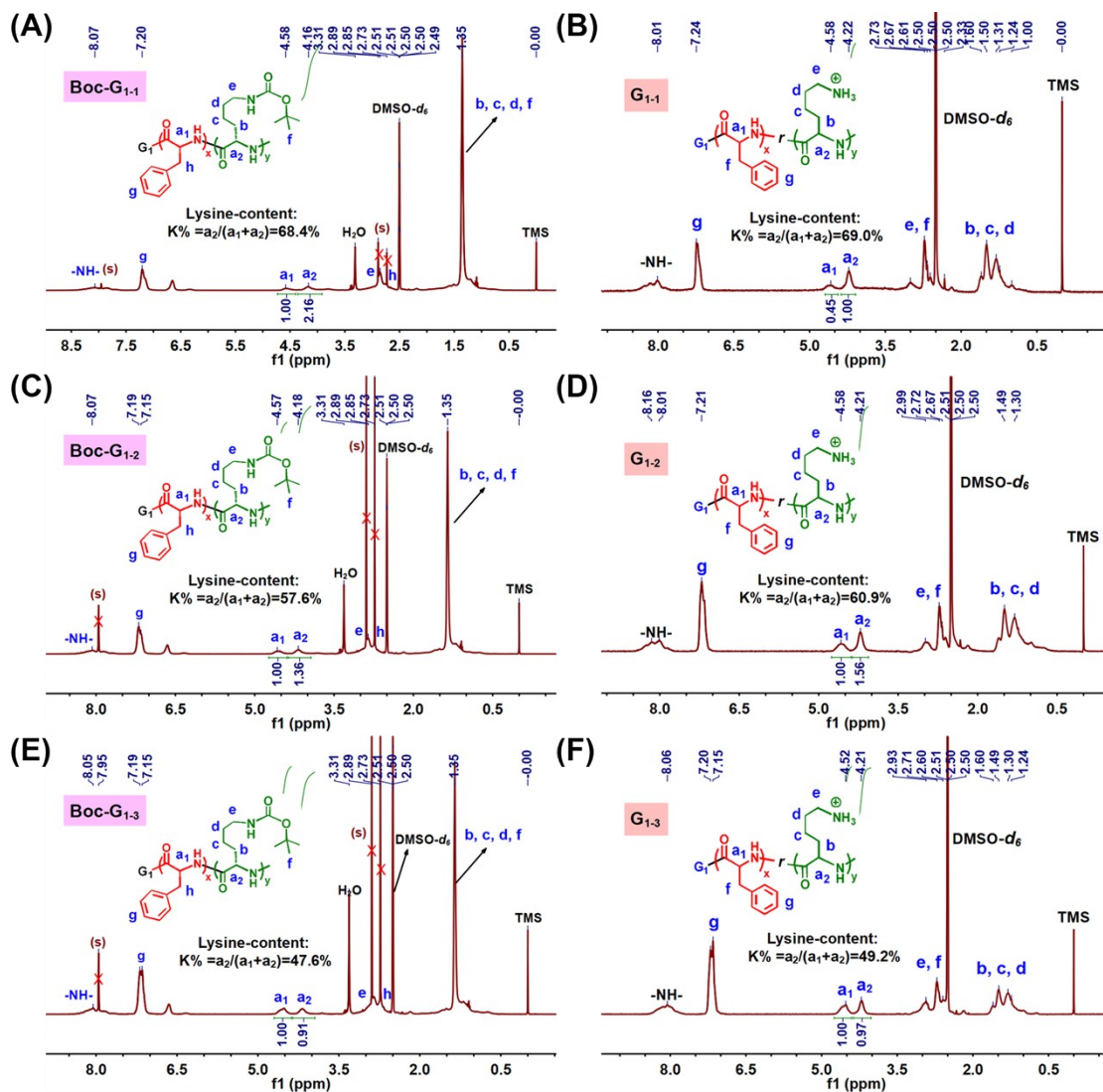
Figure S6. ^{1}H NMR spectra of star-shaped AMPs initiated by G_1-PAMAM before and after protection. (A) Boc-G_{1-1}; (B) Boc-G_{1-2}; (C) Boc-G_{1-3}; (D) G_{1-1}; (E) G_{1-2}; (F) G_{1-3}.
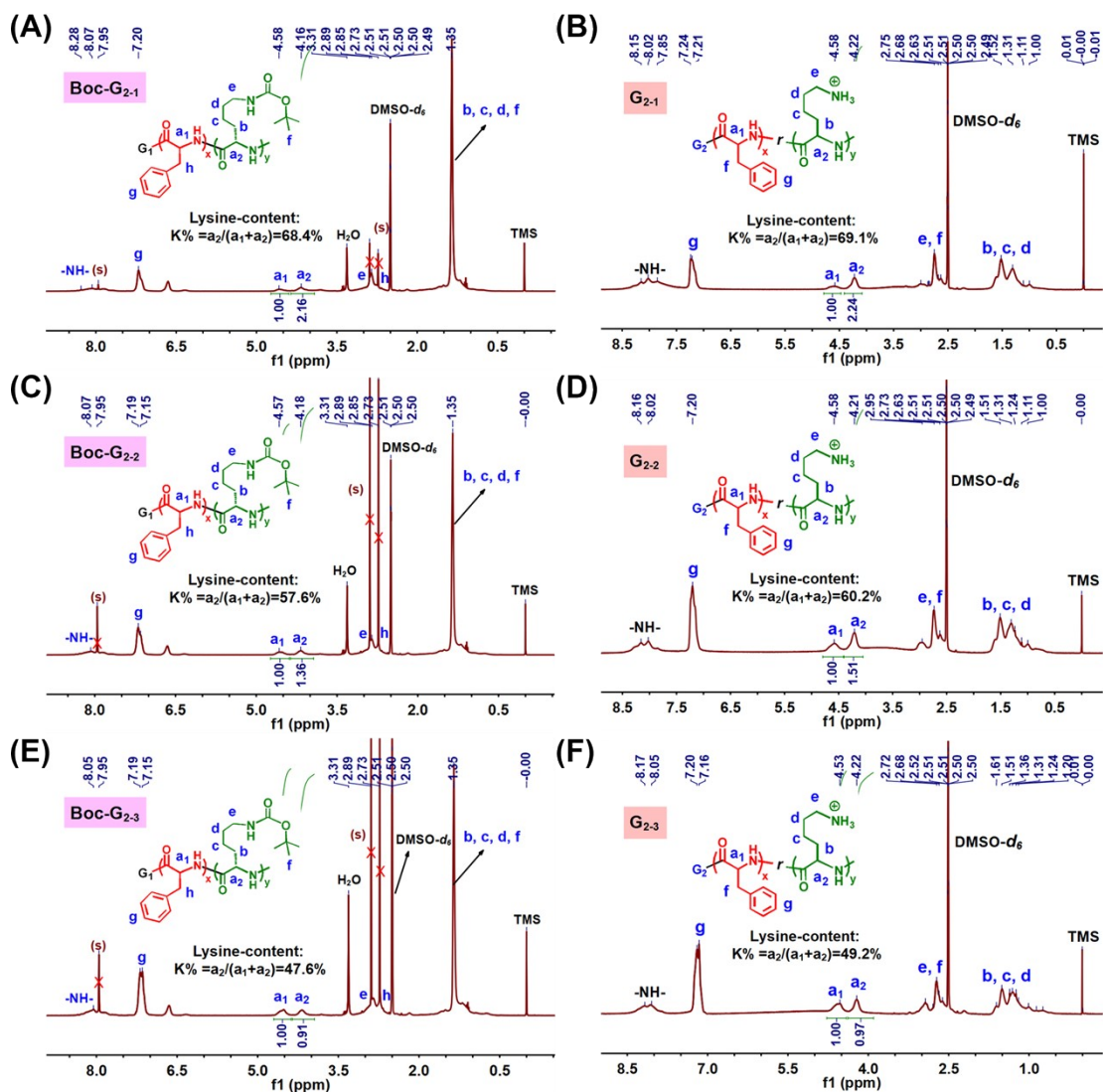
Figure S7. ¹H NMR spectra of star-shaped AMPs initiated by G2-PAMAM before and after protection. (A) Boc-G$_{2-1}$; (B) Boc-G$_{2-2}$; (C) Boc-G$_{2-3}$; (D) G$_{2-1}$; (E) G$_{2-2}$; (F) G$_{2-3}$.
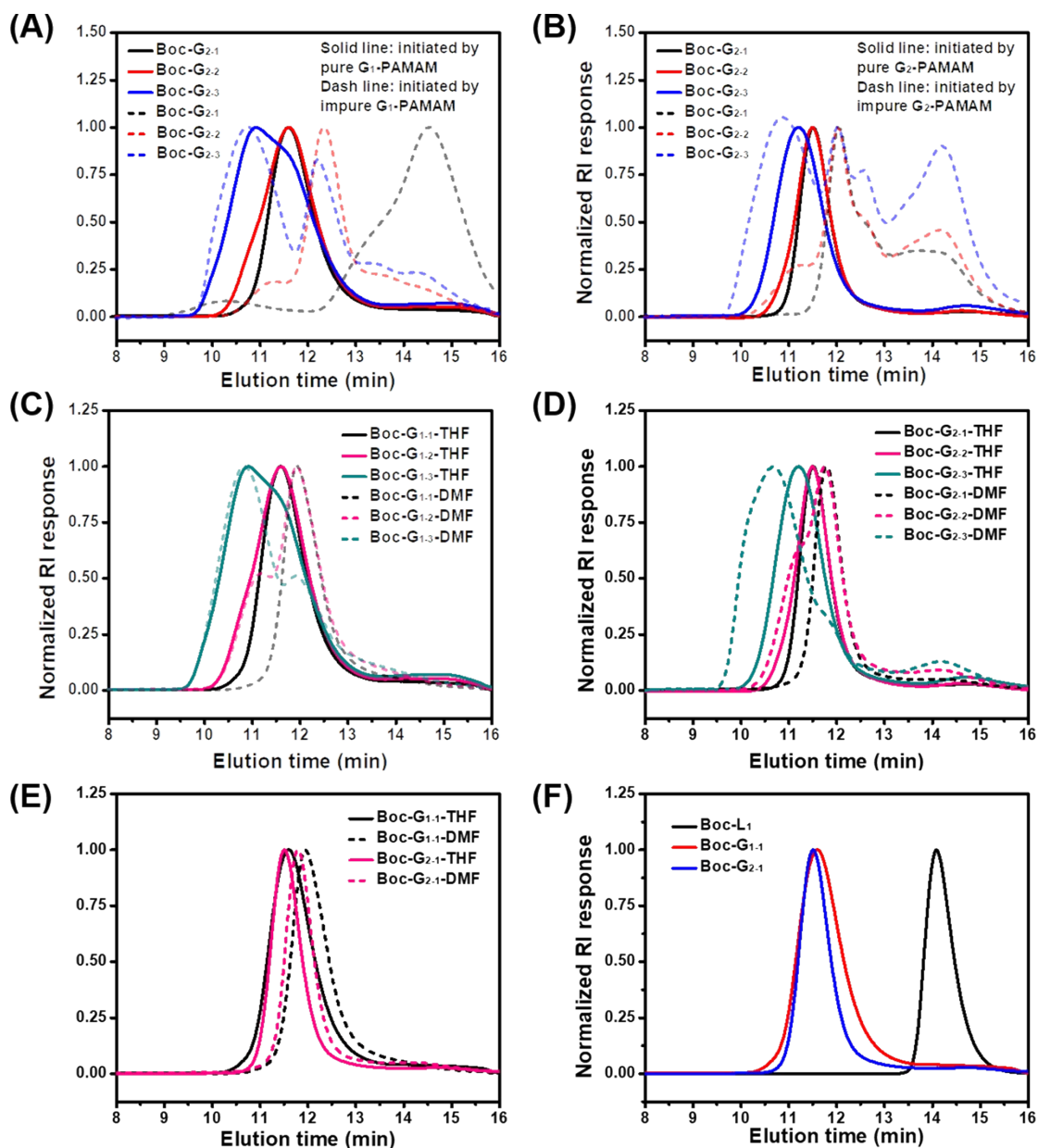
Figure S8. GPC data of the obtained Boc-AMPs. The influence of purity of G1-PAMAM and G2-PAMAM on polymerization is given in (A) and (B); The influence of solvent on polymerization is shown in (C)-(E); The GPC data of AMPs with 70% lysine content is expounded in (F).
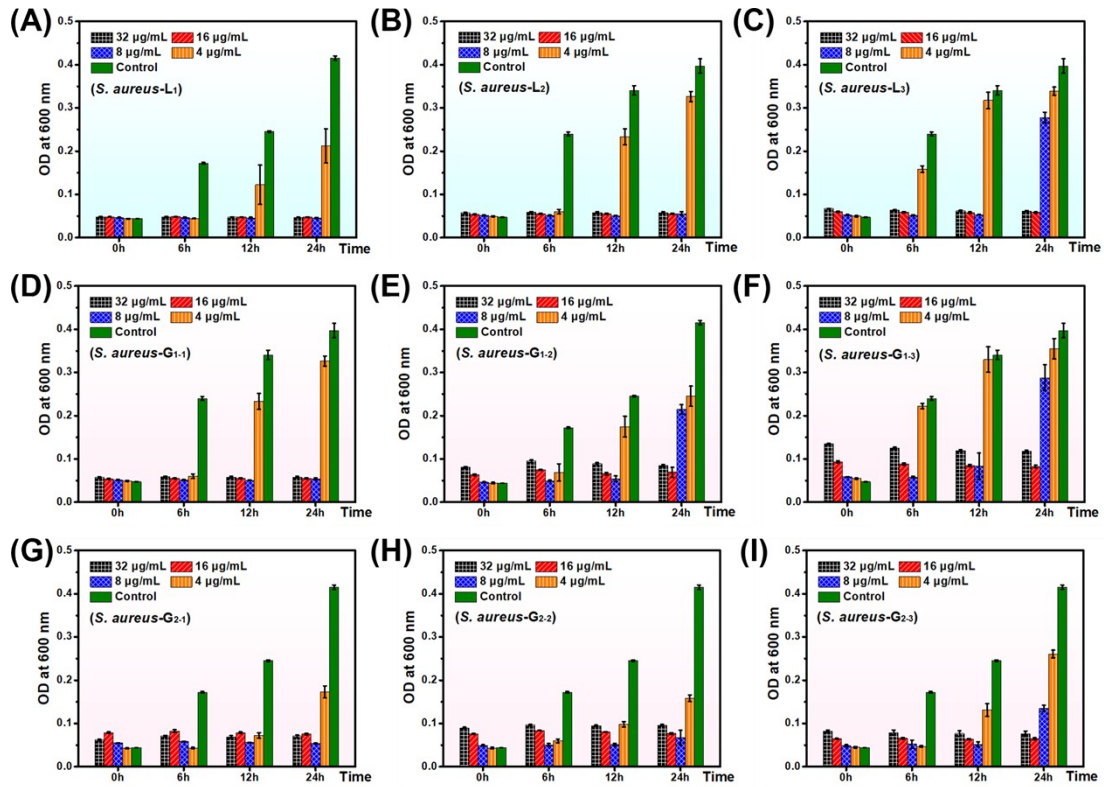
Figure S9. MICs of Linear and star-shaped AMPs against *S. aureus*. (A) L1; (B) L2; (C) L3; (D) G1-1; (E) G1-2; (F) G1-3; (G) G2-1; (H) G2-2; (I) G2-3;
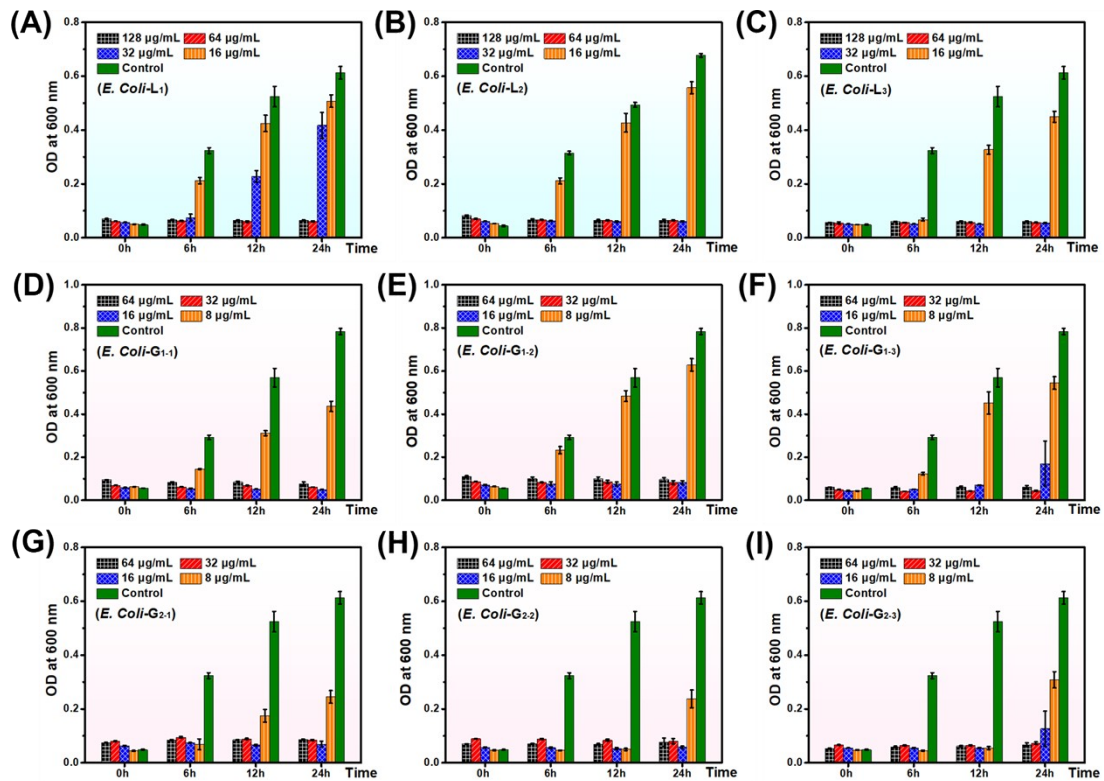

Figure S10. MICs of Linear and star-shaped AMPs against *E. Coli*. (A) L1; (B) L2; (C) L3; (D) G1-1; (E) G1-2; (F) G1-3; (G) G2-1; (H) G2-2; (I) G2-3;
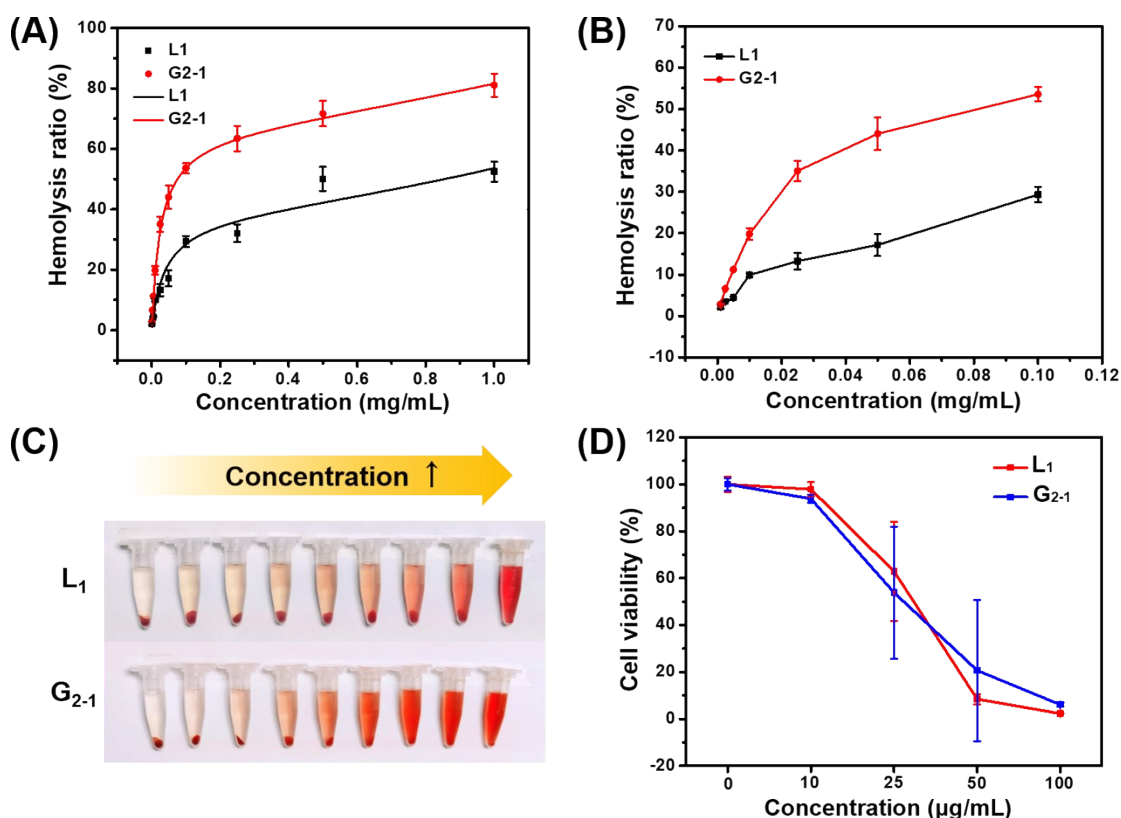
Figure S11. Biocompatibility of Linear and star-shaped AMPs against fresh rabbit red blood cells and L929 murine fibroblasts cells in solution. (A) Hemolysis data of L_1 and G_{2-1} from 1 µg/mL to 1000 µg/mL; (B) Hemolysis data of AMPs from 1 µg/mL to 100 µg/mL that enlarged from Figure A; (C) Representative pictures of Hemolysis assays corresponding to Figure A; (D) CCK-8 cytotoxicity assays.

References

1   N. J. Greenfield, *Nat. Protoc.* 2006, **1**, 2876-2890.

2   J. A. Morrow, M. L. Segall, S. Lund-Katz, M. C. Phillips, M. Knapp, B. Rupp and K. H. Weisgraber, *Biochemistry*, 2000, **39**, 11657-11666.

3   R. Baumgartner, H. Fu, Z. Song, Y. Lin and J. Cheng, *Nat. Chem.*, 2017, **9**, 614-622.

4   Z. Song, H. Fu, R. Baumgartner, L. Zhu, K. C. Shih, Y. Xia, X. Zheng, L. Yin, C. Chipot, Y. Lin and J. Cheng, *Nat. Commun.*, 2019, **10**, 5470.

5   Y. Wu, D. Zhang, P. Ma, R. Zhou, L. Hua and R. Liu, *Nat. Commun.*, 2018, **9**, 5297.

6   J. R. Kramer and T. J. Deming, *Biomacromolecules*, 2010, **11**, 3668-3672.